Proceedings of the 2006 IEEE International Conference on Robotics and Automation
Orlando, Florida - May 2006

A Rapidly Prototyped 2-Axis Positioning Stage for Microassembly Using Large Displacement Compliant Mechanisms

A. M. Hoover, S. Avadhanula, R. E. Groff, Ronald S. Fearing
University of California, Berkeley, CA 94720 USA
{ahoover, srinath, regroff, ronf}@eecs.berkeley.edu

***Abstract*— Compliant mechanisms provide an attractive alternative to conventional rigid mechanisms in the design of ultra low-cost precision positioning systems. The desirable performance characteristics of these mechanisms including freedom from backlash, long life, light weight, and ease of fabrication/assembly make them an ideal solution to the problem of inexpensive precision positioning for microassembly. This paper presents a design for a 2 axis precision positioning system which makes use of large displacement compliant mechanisms, a room temperature and pressure molding fabrication process, commodity hardware, and a piecewise linear interpolation compensation scheme to achieve positioning performance suitable for automated assembly of sub-centimeter robotic and mechatronic devices.**

I. Introduction

There is a trend toward miniaturization in many areas of industry. Miniaturized mechatronic systems and measuring devices of centimeter and sub-centimeter scale are now being developed in many sectors including information technology, aerospace, and medicine. The manufacturing equipment used to produce these products, however, is often big, inflexible, and economically inefficient. Recently, there has been a trend away from costly conventional methods (which sometimes require clean rooms, extensive human intervention and skill, and long lead times) toward small-scale and cost-efficient prototyping and production facilities called micro-factories [14]. Although there have been some impressive developments recently in these manufacturing techniques, they are still limited by their lack of affordability and accessibility [15]. Particularly during the design stage where many ideas will be tested and discarded, the development process of sub-centimeter scale mechatronic devices could be greatly enhanced with a rapid prototyping system that is flexible enough to automatically manufacture such devices in a cost-effective manner.

The objective of our research is to create a complete desktop-sized system capable of automated assembly and rapid prototyping of sub-centimeter scale robots and mechatronic devices including structural assembly, attachment of actuators and sensors, intelligence, and integrated wiring. The system must also utilize appropriate technology so as to be assembleable and operable by someone with limited technical resources and training and should be capable of being produced in the form of a kit of parts costing less than $1000 USD. One further requirement of the system is that it be entirely re-distributable, i.e. it must be possible for the end-user to easily copy custom parts (or the mechanisms used to create such parts), standard parts must not be single-sourced, and all required software must be free/open source. One possible configuration of such a system consisting of a two-axis positioning stage, computer vision, and and orthogonal gripper is pictured in figure 1.

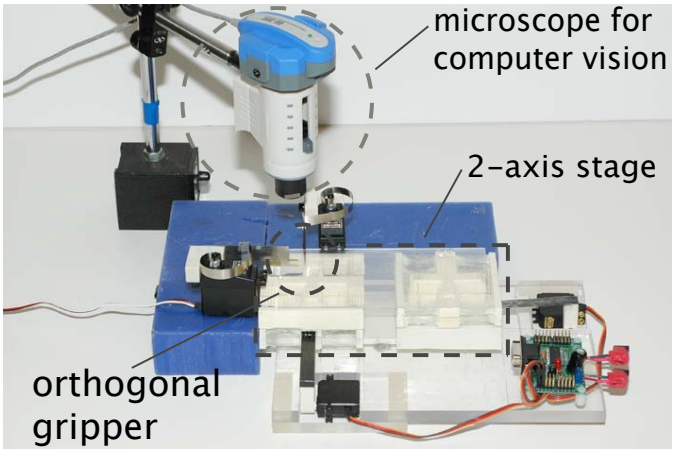

Fig. 1. Concept for ultra low-cost desktop microassembly system utiltizing an orthogonal gripper system similar to the system described in [7]

Previous work in the area of automated microassembly has relied heavily on labor/capital intensive processes such as MEMS processes or expensive commercial technology including piezoelectric actuation schemes and/or precision positioning systems. For example, the Orthotweezers technology described in [6] by Fearing, et al. at the University of California, Berkeley relies on expensive, high precision positioning stages and linear stepper motors for three axis positioning of micro-parts and piezoelectric actuation for gripping with semiconductor strain gages for force feedback. In addition to assembling millirobotic structures, microassembly systems are being developed to enable automated assembly of hybrid microsystems - systems consisting of integrated optical, fluidic, or power devices typically fabricated using MEMS processes. These systems, however, also generally rely on conventional expensive, high precision stepper and servo motors and some require additional vacuum systems for gripping and manipulation [16].

As a starting point for the system envisioned above, we

0-7803-9505-0/06/$20.00 ©2006 IEEE

propose an unconventional design for a two-axis micro-positioning system using compliant mechanisms, commercially available commodity hardware, and existing open source software.

II. Stage Design Concept

We began by determining the quantitative constraints on our design from high level requirements. The first consideration was the range of our positioning system and is a result of the size of the structures we are interested in producing. Assembly operations for sub-centimeter scale mechatronic devices including placement, wiring, and potentially folding of 2 dimensional structures will require a planar workspace at least 2-3 times larger than the structure itself, necessitating a linear range of at least several centimeters in both x and y directions. Secondly, handling of irregularly shaped small parts requires the attachment of a regularly shaped handling block for manipulation. Successful manipulation of micro-parts using 100μm x 200μm x 75μm solder-coated silicon blocks was demonstrated in [7]; to achieve similar or better results, the resolution of our positioning system should be less than 100μm. Thirdly, the constraint of a system cost of less than $1000 USD significantly limits our choice of hardware and software to hobby-grade actuators and control hardware and free or very inexpensive software. The fourth consideration was system size. A true desktop micro factory system need be no larger than 2 orders of magnitude larger than the parts being manipulated, thus dictating the overall size of our system to be on the order of centimeters or tens of centimeters. Finally, we sought to apply the guiding principle of modularity to all aspects of the design. Designing the stage as an assembly of modules reduces the number of unique parts and mates the user will be required to handle. This reduction is a well-established principle of design for assembly [10] and will greatly increase the user's chances of building and assembling a functional system.

Before arriving at the current design concept, several conventional positioning options were examined. Components of these options can be divided into two categories - bearing mechanisms and actuators. In the bearing mechanism category conventional precision linear bearings utilizing dovetail slides, ball, or crossed roller bearings were eliminated based on the combination of friction/wear characteristics and cost. Other options such as air bearings also proved too expensive with the added disadvantage that they require a very clean source of air our users cannot be expected to provide. Existing actuator technologies including precision linear stepper motors, linear induction motors, and piezoelectric actuators were also eliminated - piezoelectric for cost and range limitations, and precision linear stepper and induction motors based on cost constraints alone.

The elimination of conventional mechanical bearing options left us with the design choice of compliant mechanisms. Compliant mechanisms (one common class of which is the flexure or living hinge) are an appropriate choice for precision machinery since they require no lubrication, can be designed for effectively infinite working life, and do not exhibit backlash commonly seen in conventional mechanisms [4]. Disadvantages of compliant mechanisms are that they can be difficult to analyze and tend to have limited useful range. However, for our purposes, compliant mechanisms represent a excellent design option because they can take different forms - distributed compliance of long flexures as seen in many MEMS structures and discrete compliance as in flexural approximations of hinges or pin joints in linkages [5]. Additionally, and quite significantly, compliant mechanisms can be easily and cheaply constructed from inexpensive polymers, the high mechanical strain limits of which yield larger displacements for a fixed flexure length than other materials such as metals. The use of polymers also allows us to take advantage of molding in our construction processes. The simplicity of the room temperature and pressure molding process and the ease of replication of molds goes a long way toward making the design easily reproducible and re-distributable without requiring special technology or skilled labor.

Next, the unfeasibility of conventional precision actuators as a result of cost constraints pointed to a need for small, inexpensive, but relatively high resolution actuators and corresponding controller hardware. The proposed solution combines JR DS368 miniature digital RC servo motors and the PicoPic^{TM} servo controller available from Picobotics Inc. The DS368 motor provides 0.374 Nm of torque and less than 1μs of deadband over 120^o of range giving a theoretical resolution of 8.5μm per step for a 5cm linear range. It is also available from several sources for approximately $60 USD. The PicoPic servo controller provides 16 bit pulse width modulation resolution and servo commands with 1 μs resolution, 20 servo channels, can be programmed in any language that can send commands over a PC serial port, and costs $35 USD. This combination of actuators and controller easily meets cost and resolution requirements with the added advantage that the radio controlled vehicle industry is large and the RC servo interface is standardized, potentially giving the end user additional choice according to their application.

A. Stage Design and Fabrication

Given that our constraints have placed us in a design space in which compliant mechanisms are an appropriate solution, for our application we seek a design which is compliant in a desired direction and stiff in the orthogonal directions. One such structure which is commonly seen in MEMS designs is the folded flexure. The folded flexure consists of essentially two guided cantilever beams joined at one end by a truss with the opposite ends fixed one to ground and the other to a translating body. A typical design consists of four such folded flexures attached one to each corner of a rectangular platform with two rigid trusses spanning the folded flexures on opposite sides of the moving platform. This configuration ideally constrains the platform to a single linear translational degree of freedom. Each folded flexure can be considered as two guided cantilever beams connected in series with the resultant transverse and lateral spring constants given by:

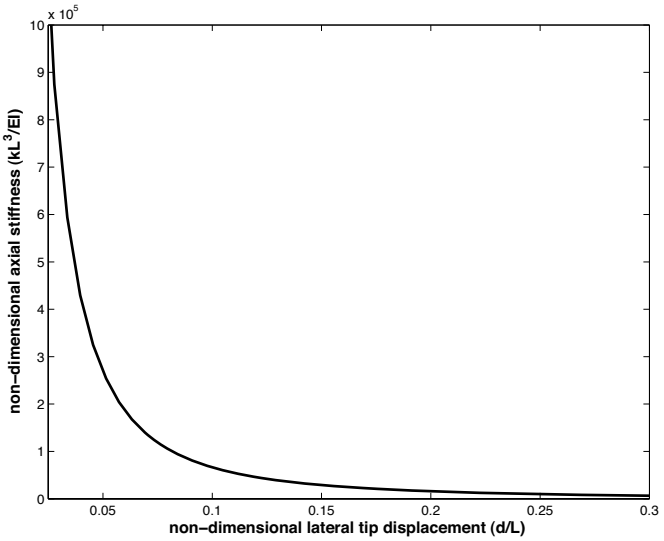

Fig. 2. Non-dimensional axial stiffness as a function of lateral tip displacement for a guided cantilever beam. Axial stiffness drops off dramatically with lateral displacement, leading to coupling of the stage's two axes of motion at large displacements.

$$k_x = \frac{2Ebh^3}{L^3} \tag{1}$$

$$k_y = \frac{2Ebh}{L} \tag{2}$$

The corresponding maximum strain occurs at the surfaces near the ends of the beams and is given by:

$$\epsilon = \frac{3\delta b}{L^2} \tag{3}$$

where δ is the lateral displacement of the beam tip, and b is the width of the beam. However, it is important to note the axial spring constant in Eq. 2 is only valid for a nominally straight beam. Solving the elastica allows us to plot the relationship between axial spring constant and transverse tip displacement to get a better understanding of how the axial spring constant changes with lateral tip displacement. This relationship is show in figure 2. The sharp drop in axial spring constant with an increase in lateral displacement indicates the flexures will not be well behaved at large displacement. This issue will be addressed later in our discussion of static nonlinearity compensation at which point we will show it is possible to compensate for this effect (and other nonlinearities) without explicitly applying the solution to the elastica. We note that the spring constant for a full suspension consisting of 4 folded flexures will simply be four times the spring constant for a single folded flexure since the flexures act in parallel.

Polyethylene terephthalate (PET) was chosen for the flexure material based on its desirable strain properties and the lengths of the flexures were calculated from Eq. 3 using a desired displacement of $\pm$20mm and a conservative maximum elastic strain estimate of 1% for PET. The design parameters for one single DOF bearing module are given in Table I. Lastly,

TABLE I

TABLE OF DESIGN PARAMETERS FOR ONE SINGLE DOF BEARING MODULE

Parameter	Value	Units
h	100	μm
b	5	mm
L	25	mm
l	75	mm
w	75	mm
flexural modulus of PET	1000	MPa
spring constant, k	3.2	N/m
actuation force, F	0.128	N

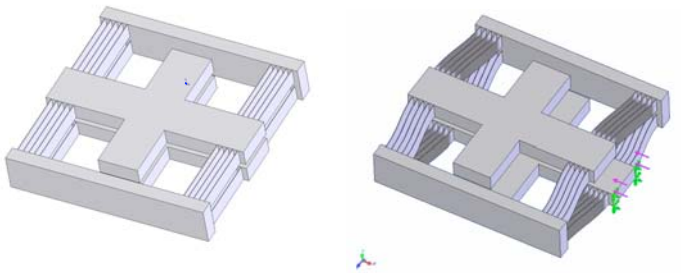

(a) Undeflected 1 DOF Module (b) Deflected 1 DOF Module

Fig. 3. Single Degree of Freedom Bearing Module

in an effort to maximize torsional stiffness about the y axis and to allow for easier actuation, we have reconfigured the conventional folded flexure design into a 3D configuration that places one flexure of the folded structure directly above the other. With the structure no longer planar, access to the moving platform for actuation was improved, range of motion became less limited by geometry, and torsional stiffness about the y axis was significantly improved by moving all flexures as far from the center of rotation as possible. Multiple parallel flexures were used to increase stiffness without raising the overall maximum strain experienced by the structure [17]. A simplified solid model of the resulting design for one single degree of freedom bearing module is pictured in figure 3 in both the relaxed and displaced positions. Two degrees of freedom are achieved by simply stacking two 1 DOF modules orthogonally to each other. Finally, two *independent* degrees of freedom were obtained by orienting two 2 DOF stacks orthogonally to each other with the lower bearing module of each stack grounded and the upper bearing modules affixed to the stage platform. The lower bearing module of each stack is then actuated independently by a grounded actuator, while the upper bearing remains passive. This is illustrated in figure 5.

The steps for fabricating single DOF bearing modules are as follows:

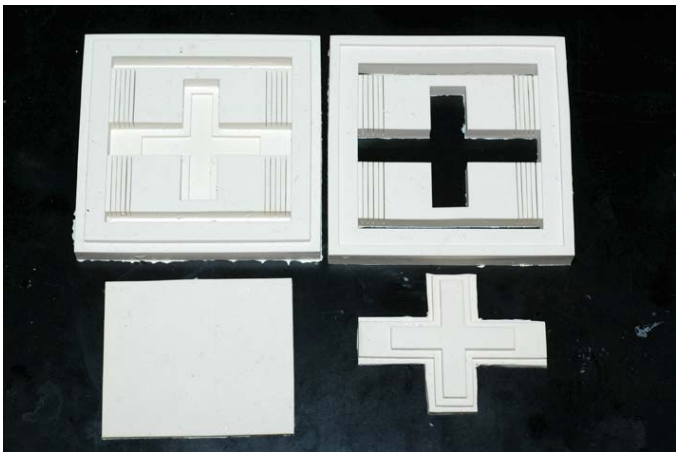

Fig. 4. Two sided PDMS mold for molding a single DOF bearing module

1) A low melting point polymer master positive mold is printed on a 3D printer.
2) Room temperature vulcanized polydimethylsiloxane (PDMS) is mixed and poured into the positive master mold and allowed to cure overnight to create a negative mold.
3) Slots in the mold for the flexures are prepped with polyvinyl alcohol (PVA) mold release agent to prevent the polyurethane from sticking excessively to the PET flexures and 5mm x 30mm strips of 100μm PET film are cut from sheets and placed into the two sides of the PDMS molds.
4) Two part Quick-Cast^{TM} polyurethane is mixed and poured into the mold: the bottom half is filled first and covered with an intermediate barrier layer of PDMS. The top half of the mold is then added and filled. The parts are left to cure for several hours.
5) Once the parts are cured, they are removed from the PDMS mold and excess polyurethane is trimmed away.

Once the PDMS molds have been made, a single DOF bearing module can be fabricated in this fashion in less than a day. Two single degree of freedom modules can be snapped together in an orthogonal orientation to create a stack with 2 degrees of freedom. Two such stacks are then snapped to a base plate (fabricated using the above process) in an orthogonal orientation and a rigid platform is affixed to the top bearing module in each stack. The result is pictured in figure 5.

In order to actuate the stage, it was first necessary to identify a compact, simple mechanism for the conversion of rotational motion into translation. Planar options such as the Peaucellier and Kempe straight line mechanisms, the kinematics of which are described in [12], were considered but ultimately rejected based on the difficulty of fabrication using short flexure hinges. A slider crank mechanism was chosen for its relative simplicity and because it's fabrication using composite links and flexural hinges has been demonstrated in [8]. For an offset slider

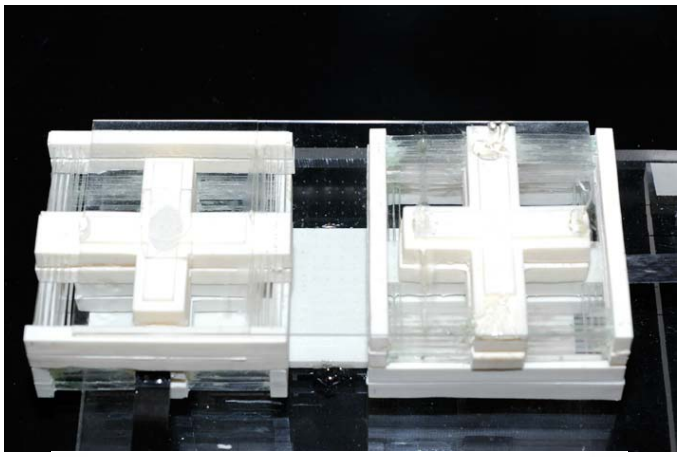

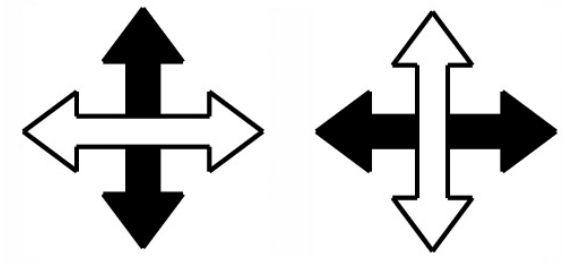

Fig. 5. Fully assembled stage with two independent degrees of freedom shown with carbon fiber actuation linkages attached. The arrows in the diagram illustrate the behavior of the four bearing modules. Solid arrows represent actuated bearing modules on the bottoms of their respective stacks. The outlined arrows are the passive modules and are rigidly connected by the top stage platform.

crank linkage consisting of links with length l_1 and l_2, the displacement, x, from center is given by:

$$x = l_1 sin\theta + \sqrt{l_2^2 - l_1^2(1 - cos\theta)^2} - l_2 \tag{4}$$

where θ is the angle of rotation of link l_1 and is half the range of the servo motor or 60^o in our case. From Eq. 4 we arrive at the dimensions give in Table II.

To design the flexures in the slider crank, we use the following relation from [1]:

$$d = \frac{E\theta_{max}h}{2\sigma_y} \tag{5}$$

where d is flexure length, h flexure thickness, and $\frac{E}{\sigma_y}$ represents the yield strain in the flexure. Again, using a conservative value of 1% for the yield strain of PET and making the flexure as thin and short as possible (the justification for which has been shown in [2]), we obtain the flexure design parameters given in Table II.

One link of the slider crank was fabricated from Quik-Cast^{TM} polyurethane using the room temperature and pressure molding process described above, while the other along with two flexure hinges and corresponding tabs for attachment were fabricated from carbon fiber and PET film using the methods described in [8]. The actuators were grounded to the base of the stage and the polyurethane link was pressed onto the splined shaft of the RC servo while the tabs at the ends of the

TABLE II

TABLE OF DESIGN PARAMETERS FOR CARBON FIBER SLIDER CRANK LINKAGES

Parameter	Value	Units
l_1	25	mm
l_2	50	mm
d	150	μm
h	12.5	μm
flexural modulus of PET	1000	MPa

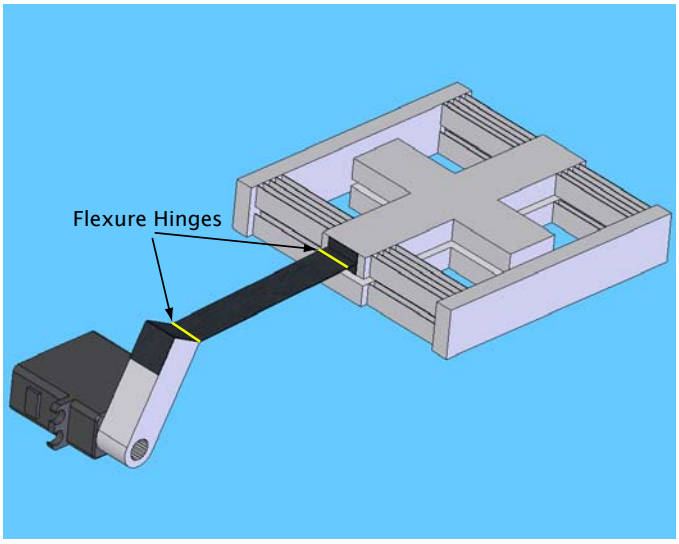

Fig. 6. Solid model of the carbon fiber/polyurethane slider crank linkage connecting the RC servo actuator to a single DOF bearing module.

carbon fiber link were glued at one end to the polyurethane link and at the other to the lower bearing module as depicted in figure 6. Care was taken not to misalign the flexures in an effort to avoid undesirable off-axis loads. The actuators were then plugged into the PicoPic controller board, and the stage was set up for performance characterization testing.

III. EXPERIMENTAL RESULTS

The measurement procedures for testing the stage made use of two setups. In the first setup, a computer-controlled desktop laser cutting machine was used to cut small dots in a sheet of paper placed on the stage. The second setup consisted of a rectilinear grid printed on paper and attached to the surface of the stage and a digital camera to capture images of the grid as the stage was commanded to different positions. Both systems made extensive use of image processing for extrapolating position data from images.

The first experiment consisted of driving each stage actuator to 10 linearly spaced command positions over its full range and cutting a small dot in a sheet of paper using the laser cutter. The result was then scanned at 2400 dpi using a document scanner. Using Matlab, the image was converted to black and white, filtered for speckle noise, and inverted. The centroid of each dot was then calculated and the resulting data point

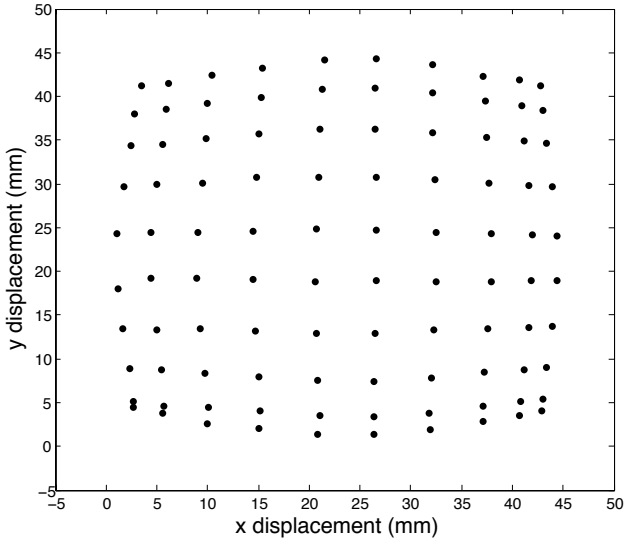

Fig. 7. Uncompensated position data

plotted. The results are plotted in figure 7. From figure 7 we note the nonlinear behavior of the position data. We know from figure 2 this behavior is expected as a result of the fact we are operating at large displacements - our displacements are on the order of 40% of flexure length while the rule of thumb for conventional precision machine design is that displacement should be no more than 5% of flexure length [13]. To compensate for this static nonlinearity a two-dimensional piecewise linear interpolation scheme similar to the work presented in [11] was chosen. Using the 10x10 grid of uncompensated data and the corresponding actuator commands, a map from desired position to actuator command was created. A simple computational routine then takes commanded stage position in and returns the corresponding actuator commands based on linear interpolation of the observed data. This approach is computationally inexpensive and provides the added advantage that the map, while not guaranteed to always be invertible, is invertible for our application. The results of applying compensation to the stage are given in figure 8. The effectiveness of the scheme can be improved further still with the addition of more data to the map. We also note that compensation necessarily results in reduced range. In this case, the compensation has limited the range to 35mm.

From the data plotted in figure 8, we can measure the distance along the x or y axis between any two points and divide that distance by the difference in actuator commands for that axis. The mean of many such measurements provided an estimate of 35μm resolution for the stage, compared with a theoretical resolution of 25μm based on a range of 35mm, the PicoPic's resolution of 1μs, and the servos' inability to respond to pulse widths smaller than 800μs and larger than 2200μs. The deviation of the observed compensated position data from linear is shown in figure 9.

The final measurement that was performed was a test of

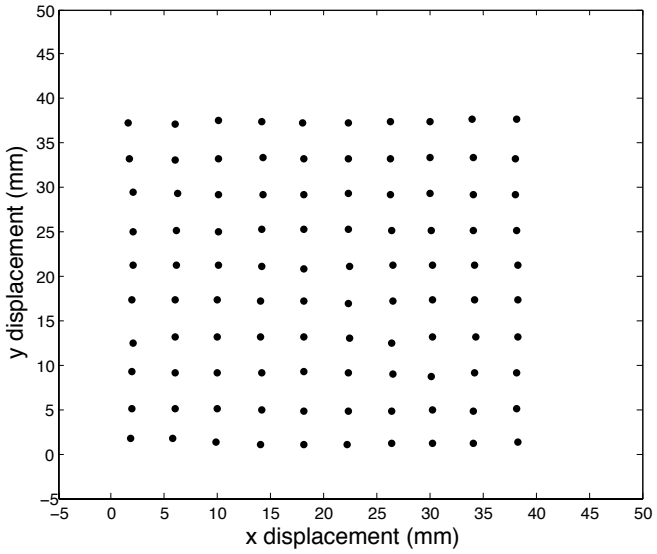

Fig. 8. Position data with piecewise linear interpolation compensation applied

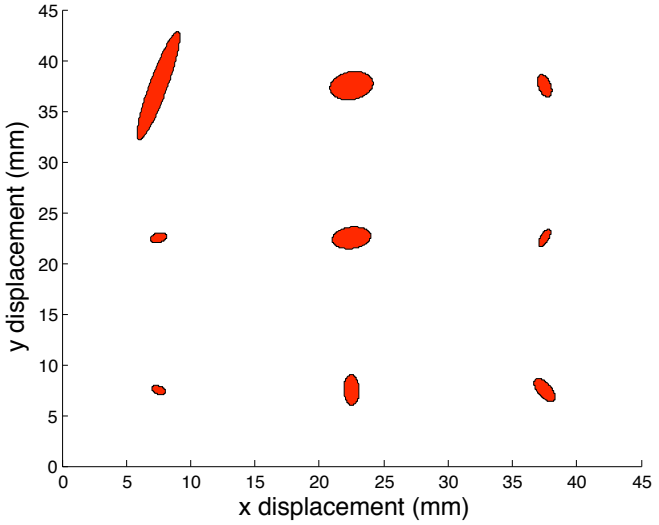

Fig. 10. Covariance ellipses scaled 20x plotted for nine stage positions with 100 samples taken at each position

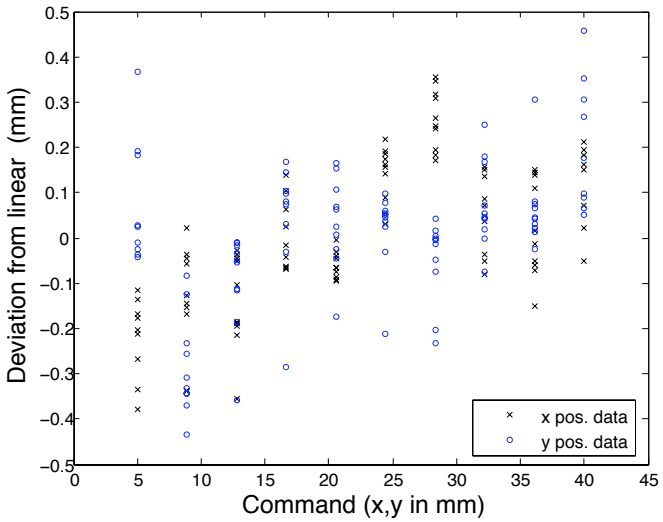

Fig. 9. Linearity of compensated position data in x and y plotted vs. commanded position

repeatability. A 3x3 grid of approximately 350μm diameter black dots spaced 15mm from each other was printed on white paper and affixed to the top of the stage. The stage was placed beneath a digital camera and commanded to each of the 9 dot positions 100 times. At each position, the stage paused and a digital image was captured by the camera. At full zoom, the camera provided 7.5μm per pixel of resolution. The resulting sequence of images was converted to black and white, filtered, and inverted and the location of the centroid of each dot was calculated for each position. That data was used to calculate the covariance at each point. A plot of the covariance ellipses scaled 20x for each of the nine positions is given in figure 10. The maximum variance in both directions occurs at the upper left (1,3) point of the plot, with a variance in x of $\pm$80μm and a variance in y of $\pm$ 250μm. The minimum variance occurs in the first column and second row (1,2) with a variance of $\pm$25μm in y and $\pm$30μm in x. Further examination of the anomolous data at the point of maximum variance showed two distinct clusters of points, potentially indicating the possibility of a mechanical defect like the action of friction between two parts or plastic deformation of compliant elements.

IV. Summary and Future Work

Using a combination of compliant mechanisms, a rapid prototyping process that includes room temperature and pressure molding of polymer structures, and commodity hardware has allowed us to design and fabricate an ultra low-cost and redistributable two axis positioning system for microassembly. The combination of mechanical design and piecewise linear compensation have allowed us to demonstrate a measured resolution of 35μm, a mean repeatability to within $\pm$125μm, and a range of 35mm, meeting or nearly meeting all of our initial design requirements. It should also be noted that combining this positioning system with passive alignment fixtures has the potential to further reduce positioning error so that it is of the same order as our resolution. These results represent the first step in developing a complete, inexpensive, and redistributable system for automated assembly of sub-centimeter scale robots and mechatronic devices. Such a system could eventually enable a cost-effective rapid prototyping paradigm that will allow users to more effectively focus their energy on novel designs for miniature robots and mechatronic devices rather than difficult assembly tasks.

Future work will include the addition of a 3rd positioning axis to allow for true 3D micro-manipulation. Issues with the current design that were not discussed here which we would like to address in future work include maximizing z axis stiffness at large displacements to avoid complications due to tilt or load bearing with the addition of a 3rd positioning

axis. As well, distributed compliance mechanisms have the potential to introduce unwanted dynamics into a system given their elastic nature. Discretely compliant mechanisms using rigid members and short flexure hinges have potential for reducing dynamic effects and may merit further investigation. We would also like to simplify the design by using the same molding process to produce the actuation linkages as was used to fabricate the bearing modules. Standardizing on this process will allow us to mold geometric mates into parts, eliminating all gluing which represents a potentially large source of error. Although Matlab was primarily used to process image data for the compensation, it should be noted that all necessary functions for the procedures described in this paper exist in the add-on image processing and numerical computing modules for the open source programming language, Python. Future work will integrate Python into the existing setup more completely and may take advantage of additional open source libraries such as Intel's OpenCV for computer vision functionality, completely eliminating the need for the precision laser cutter in the calibration process. Finally, we would like to integrate the positioning system with a gripper and a computer vision system to develop a complete microassembly system in accordance with the design objectives enumerated in the introduction.

ACKNOWLEDGEMENTS

This material is based upon work supported by the National Science Foundation under Grant No. DMI-0115091 and DMI-0423153. Any opinions, findings and conclusions or recommendations expressed in this material are those of the author(s) and do not necessarily reflect the views of the National Science Foundation (NSF). R. E. Groff is supported by the DCI postdoctoral fellowship.

REFERENCES

[1] Goldfarb, M. and J. E. Speich, "A Well-Behaved Revolute Flexure Joint for Compliant Mechanism Design," *Journal of Mechanical Design*, vol. 121, pp. 424-429, Sept. 1999.

[2] Sahai, R, E. Steltz, and R.S. Fearing, "Carbon Fiber Components with Integrated Wiring for Millirobot Prototyping" *IEEE ICRA 2005*, Barcelona, Spain, Apr. 18-22, 2005.

[3] Sahai,R, J. Lee, and R.S. Fearing, "Towards Automatic Assembly of Sub-Centimeter Millirobot Structures," *Third International Workshop on Microfactories*, Minneapolis, MN, Sept. 16-18, 2002.

[4] Howell, L. L. Compliant mechanisms, John Wiley & Sons, 2001, ISBN: 0-471-38478-X.

[5] Howell, L. L., and A. Midha, "A Method for the Design of Compliant Mechanisms with Small-Length Flexural Pivots", *ASME J of Mech Design*, vol. 116, no.1, pp. 280-290, March 1994.

[6] Thompson, J.A., and R.S. Fearing, "Automating Microassembly with Ortho-tweezers and Force Sensing," *IROS 2001*, Maui, HI, Oct. 29 - Nov. 3, 2001.

[7] Shimada, E., et al., "Prototyping Millirobots using Dexterous Microassembly and Folding," *Symp on Microrobotics, ASME Int Mech Eng Cong And Exp*, Nov. 5-10, 2000, Orlando, FL.

[8] Wood, R.J., S. Avadhanula, M. Menon, and R.S. Fearing, "Microrobotics Using Composite Materials: The Micromechanical Flying Insect Thorax," *IEEE ICRA 2003*, Taipei, Taiwan, Sept. 14-19, 2003.

[9] Slocum, A. and A. Shorya, "Fabrication, assembly and testing of a new XY flexure stage with substantially zero parasitic error motions," http://www.mit.edu/people/shorya/PHD/report.pdf.

[10] Boothroyd, G., and Dewhurst, P., *Design for Assembly Handbook*, University of Massachusetts, Amherst, 1983.

[11] Groff, R.E. "Piecewise linear homeomorphisms for approximation of invertible maps", Ph.D. Thesis, University of Michigan, April 2003.

[12] Eckhardt, H. Kinematic *Design of Machines and Mechanisms*, McGraw-Hill, New York, 1989

[13] Slocum, A. *Precision Machine Design*, Prentice Hall, 1992.

[14] International Workshop on Microfactories, Shanghai, China, Oct. 15-17, 2004; http://iwmf04.ustc.edu.cn/home.html

[15] Gershenfeld, N. "Microfinance, Microfab", http://www.forbes.com/columnists/free_forbes/2005/0425/032.html, Apr. 25, 2005

[16] G. Yang, J. A. Gaines, B. J. Nelson, "A Supervisory Wafer-Level 3D Microassembly System for Hybrid MEMS Fabrications", Journal of Intelligent and Robotic Systems, 2003, 37: pp. 43-68

[17] Moon, Y. M., B. P. Trease, and S. Kota, Design of large displacement compliant joints, in ASME Design Engineering and Technical Conference, pp. MECH34207, (Montreal), 2002.